PROCEEDINGS, Twenty-Ninth Workshop on Geothermal Reservoir Engineering
Stanford University, Stanford, California, January 26-28, 2004
SGP-TR-173

PORO-THERMOELASTIC MECHANISMS IN WELLBORE STABILITY AND RESERVOIR STIMULATION

A. Ghassemi and Q. Zhang

Department of Geology & Geological Engineering
University of North Dakota
Grand Forks, ND 58202

ABSTRACT

Some fundamental mechanisms associated with cooling/heating of the rock in the context of drilling and reservoir stimulation in enhanced geothermal systems are described. The role of temperature and pore pressure in wellbore failure and fracture width is considered using analytical and boundary element models. Results indicate that cooling induces a pore pressure drop inside the formation that tends to increase the effective stresses near the wellbore but, it reduces the total stresses in the rock near the well more significantly (decreasing the stress difference, i.e., Mohr's circle radius). Thus, cooling causes wellbore stability with respect to shear failure and instability with respect to tensile failure. Consequently, one often observes tension cracks whereas compressional wellbore breakouts may be absent. The cooling mechanism is useful in stimulation by cold fluid injection to enhance fracture permeability. Cooling increases joint aperture and the stress intensity at the fracture tip leading to crack growth. As a result, fracture slip may occur leading to permeability enhancement. On the other hand, increased pore pressure in the rock matrix reduces fracture width.

INTRODUCTION

Coupled thermal and poro-mechanical processes play an important role in a number of problems of interest in geomechanics such as stability of boreholes and permeability enhancement in geothermal reservoirs or high temperature petroleum bearing formations. when rocks are heated/cooled, the bulk solid as well as the pore fluid tend to undergo a volume change. A volumetric expansion can result in significant pressurization of the pore fluid depending on the degree of containment and the thermal and hydraulic properties of the fluid as well as the solid. The water trapped in the pores may undergo pressure increases on the order of 1.5 MPa per degree Kelvin during heating for conditions typical of earth's upper crust (Williams and McBirney 1979). The net effect is a coupling of thermal and poromechanical, and chemical processes when developing a geothermal reservoirs. These processes occur on various time scales and the significance of their interaction and coupling is dependent upon the problem of interest. For example, in drilling operations there is a strong coupling between thermal and poromechanical effects that has significant impact on the stress/pore pressure distribution around the wellbore and thus hole failure and fracture initiation. This is caused by the contrast in thermal and hydraulic diffiusivities of the rock and also because drilling through rock takes less time than the characteristic time $\frac{a^2}{c^f}$, where a is the radius of the well and c^f is the fluid diffusivity. On the other hand in hydraulic fracturing, the evolution of the fluid-rock mechanics coupling evolves rapidly (on the scale of minutes, hours to possibly days) compared to thermal pro-cesses, thus the thermal effects have little effect on the fluid-mechanical processes involved in fracture propagation. However, During a long term injection phase (time scale of years), the thermo-mechanical coupling can no longer be neglected. Accordingly, different levels of coupling are necessary when studying wellbore failure, fracture propagation, and fluid circulation.

PORO-THERMOELASTICITY

A poro-thermoelastic approach combines the theory of heat conduction with poroelastic constitutive equations (Biot, 1941), coupling the temperature field with the stresses and pore pressure. The governing equations of porothermoelasticity are (McTigue, 1986; Palciauskas and Domenico, 1982):

Constitutive equation (tension positive):

$$\Delta\varepsilon_{ij} = \frac{\Delta\sigma_{ij}}{2G}, \quad i \neq j \tag{1}$$

$$\Delta\varepsilon_{kk} = \frac{\Delta\sigma_{kk}}{3K} + \frac{\alpha\Delta p}{K} + \beta_s^{'}\Delta T \tag{2}$$

$$\sigma_{ij} = 2G\varepsilon_{ij} + (\frac{2G\nu}{1-2\nu}\varepsilon - \alpha p + K\beta_s^{'}T)\delta_{ij} \tag{3}$$

$$\Delta\zeta = \frac{\alpha}{3K}\Delta\sigma_{kk} + \frac{\alpha\Delta p}{BK} - \phi_0(\beta_f - \beta_s^{''})\Delta T \tag{4}$$

Equilibrium equations:

$$\sigma_{ij,j} = 0 \tag{5}$$

Darcy's law:

$$v_i = -\frac{k}{\mu}p_{,i} \tag{6}$$

Continuity equations:

$$\frac{\partial\zeta}{\partial t} + q_{i,j} = 0 \tag{7}$$

Fourier: $$q_i^T = -k^T T_{,i} \tag{8}$$

where σ_{ij} denotes the components of the total stress tensor, ζ is the variation of the fluid content per unit volume of the porous material, and ε_{ij} are the components of the strain tensors related to the solid displacements u_i by $\varepsilon_{ij} = \frac{1}{2}(u_{i,j} + u_{j,i})$. The constant K is the rock's bulk modulus; B is Skempton's pore pressure coefficient; $\alpha = \frac{3(\nu_u-\nu)}{B(1-2\nu)(1+\nu_u)}$ is Biot's effective stress coefficient; $\beta_s^{'}$ is the volumetric thermal expansion coefficient of the bulk solid under constant pore pressure and stress; and $\beta_s^{''}$ and β_f represent volumetric thermal expansion coefficients of the solid matrix and the pore fluid, respectively. The former, $\beta_s^{''}$, reflects the phenomena engendered by the internal pore geometry and stress fields that are caused by a temperature change; it may be considered equal to $\beta_s^{'}$ (henceforth denoted by β_s) if the change in temperature is not expected to change porosity, ϕ_o. $\kappa = \frac{k}{\mu}$, in which k is dynamic permeability and μ is the fluid viscosity; k^T is the thermal conductivity and c^T is the thermal diffusivity. The above equations can be combined to yield a set of field equations:

$$G\mathbf{u}_{i,jj} + \frac{G}{1-2\nu}\varepsilon_{kk,i} - \alpha\mathbf{p}_{,i} - \beta_s K T_{,i} = \mathbf{0} \tag{9}$$

$$\frac{1}{M}\frac{\partial p}{\partial t} = \frac{k}{\eta}p_{,ii} - \alpha\frac{\partial\varepsilon_{kk}}{\partial t} + D\frac{\partial T}{\partial t} \tag{10}$$

$$\frac{\partial T}{\partial t} = c^T T_{,ii} \tag{11}$$

with $M = \frac{2G(\nu_u-\nu)}{\alpha^2(1-2\nu)(1-2\nu_u)}$ is Biot's modulus, G is shear modulus, and $D = \alpha\beta_s + \phi(\beta_f - \beta_s)$. It should also be noted that for most rocks, heating/cooling produces thermal stresses and changes pore pressure, but stress and pressure changes do not significantly alter the temperature field so that the latter is not coupled to the equations for the pore pressure and solid displacements.

Poro-Thermoelastic BEM

A few analytical procedures have been developed and used to solve rock mechanics problems of interest involving coupled thermal and poromechanical problems (Delaney, 1982; Wang and Papamichos, 1994; Li *et al.* 1988; Ghassemi and Diek, 2002). However, often times many problems are not amenable to analytical treatment and need to be solved numerically. The boundary element method (BEM) or the boundary integral equation formulation also has proven effective for the poroelastic and thermoelastic problems (e.g., Ghassemi & Roegiers, 1996; Cheng *et al.* 2001; Ghassemi *et al.* 2001, 2003). The *fictitious stress (FS) and the displacement discontinuity (DD)* techniques are indirect boundary element methods. The former is based on the fundamental solutions to the problems of fluid/heat source and point force in an infinite solid; the latter utilizes similar singular solutions with a point DD used instead of a point force. Both of these techniques have been combined herein to enable treatment of a problems involving wellbores and cracks. For the sake of brevity, the details of the formulation are not presented. The interested reader is referred to (Ghassemi and Zhang, 2004).

APPLICATIONS

Consider a borehole with a radius $R = 0.1$ m in a reservoir that is at a temperature of 200^oC. The wellbore wall is suddenly cooled by water and maintained at 80^oC. For clarity

of presentation and investigation of the role of temperature, only induced stress and pore pressures are studied. Thus, pore pressure and stress loadings are not considered. Due to symmetry only a quarter of the wellbore is modeled using 10 elements. For each computation, the time is divided into 10 steps with the value of increment adjusted accordingly. The input parameters are shown in Table 1. Figures 1-4 illustrate the profiles of temperature, induced pore pressure, induced tangential stress, and induced radial stress around the wellbore. Analytical results are also shown for comparison. As can be observed, the numerical results are in agreement with the analytic solution (e.g., Li *et al.* 1998). Figure 1 shows the transient temperature distribution; it is typical of a conductive heat transfer situation. The formation is gradually cooled off when the borehole temperature is suddenly reduced. Figure 2 is the distribution of induced pore pressure; a significant pressure drop is generated near the borehole at early times. With increasing time, the pore pressure peak is reduced and moves away from the well where it gradually recovers the original state. Figure 3 presents the thermally induced tangential stress. With cooling, a significant tangential tensile stress is induced around the wellbore. This is caused by the tendency of the rock to shrink near the borehole wall. Away from the borehole wall, the magnitude of the induced tensile stress decreases and changes its sign at some point inside the formation i.e., turns into a compressive stress. This is because the shrinkage of the material near the borehole tends to pull on the outer rock, thus inducing a compressive stress. The compressive zone gradually moves away from the borehole and is diminishes in magnitude. Figure 4 illustrates the thermally induced radial stress; a significant radial tensile stress peak is produced inside the formation. At later times, the tensile stress zone moves inside the formation while the magnitude of the "peak" increases.

We now solve a crack problem using the DD part of the model. Consider a crack of length 2L in a reservoir that is at a temperature of 200^{o}C. The crack surfaces are suddenly cooled by water and maintained at 0^{o}C (shown in Figure 5). This problem of fracture pressurization by a cooler fluid under pressure P may be decomposed into three subproblems corresponding to three fundamental modes of loading: a normal stress loading, a pore pressure loading, and a temperature loading:

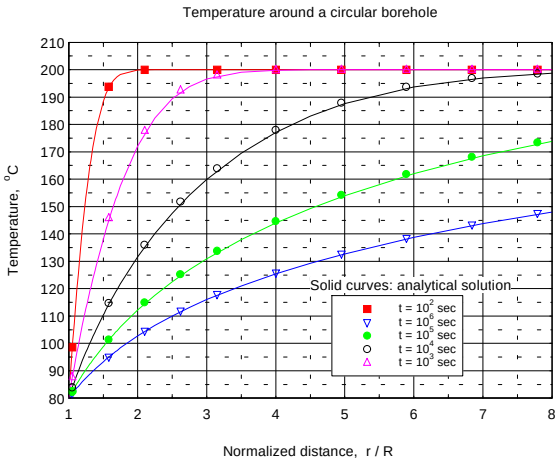

Figure 1: Temperature distribution around the well for various times.

	σ_n	$p(x,t)$	$T(x,t)$
$Mode1$	$PH(t)$	0	0
Mode 2	0	$PH(t)$	0
Mode 3	0	0	$T_1H(t)$

where $H(t)$ denotes the Heaviside step function. The initial conditions for each sub-problem are zero stress, pore pressure, and a temperature of T_0 everywhere. Due to symmetry, only a half of the crack is modeled using 10 elements. For each computation, the time is divided into 10 steps with the value of increment adjusted accordingly. The input parameters are shown in Table 1.

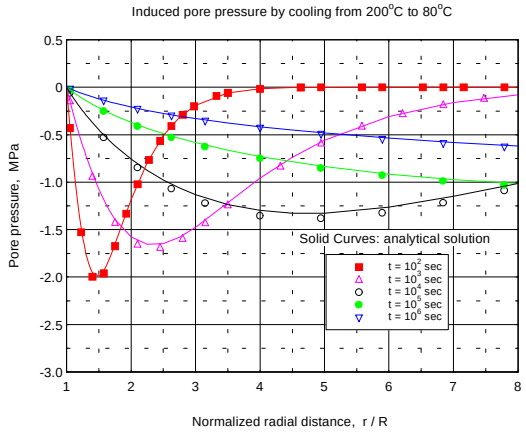

Figure 2: Pore pressure distribution around the wellbore.

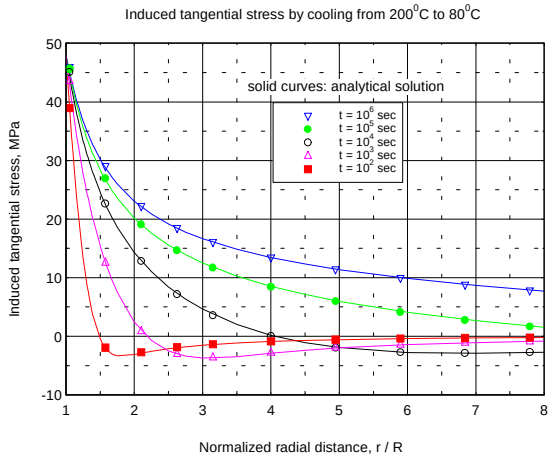

Figure 3: Tangential stress distribution around the wellbore.

Table 1. Input Parameters			
G	shear modulus	$1.50e04$	MPa
ν, ν_u	Poisson's ratio	$0.25, 0.33$	
K_s	solid modulus	$4.50e04$	MPa
C	heat capacity	790.0	J/(kg·^oC)
c^T	thermal diff.	$5.10e$-6	m^2/ sec
c^f	fluid diff.	$6.16e$-5	m^2/ sec
β_s	solid exp coef.	$2.40e$-5	m/^oC
β_f	fluid exp. coef.	$3.00e$-4	m/^oC
k	permeability	$4.053e$-7	darcy

The result of Mode 1 loading is shown in Figure 6. This mode of loading is responsible for the opening of the fracture. At time $t = 0^+$, the fracture opens according to the well known solution of Sneddon (1946) with undrained material properties (Detournay & Cheng, 1991):

$$W = -\frac{2pL(1-\nu_u)}{G}\left(1 - \frac{x^2}{L^2}\right) \qquad (12)$$

As time increases the crack opening also increases, approaching the steady-state solution given by the previous equation with drained material properties. This stage of rock deformation is referred to as the drained stage. The crack opening is a maximum at this stage reflecting the softer material behavior.

The fracture response in Mode 2 is illustrated in Figure 7. A purely thermoelastic formulation cannot consider this loading mode which causes the crack to close progressively, starting from a zero value and reaching a final normalized maximum closure value of 0.22 given by $(\hat{D}_n)_{max} = 2\eta(1-\nu)$, where η is the poroelastic stress parameter $\eta = \frac{\alpha(1-2v)}{2(1-\nu)}$: [0-0.5], and $(\hat{D}_n)_{max} = \frac{D_n(0,t)G}{PL}$. Physically, the two crack surfaces cannot overlap, this closure is possible only if the crack remains open, under appropriate stress, pore pressure and temperature. The numerical model overestimates the fracture opening by about 5 per cent. This may be attributed to the use of constant elements. A comparable error was also observed when modeling pressurized cracks in elastic media using constant elements (Crouch and Starfield, 1983).

The Mode 3 fracture response as a function of time is illustrated in Figure 8 . It can be seen that cooling the crack surfaces and the surrounding rock results in opening of the fracture. This is the opposite of the effect of fluid invasion into the rock mass that tends to close the crack.

The fracture opening approaches the asymptotic value, the latter is obtained using an approach similar to the poroelastic case (Zhang, 2004). This consists of applying the

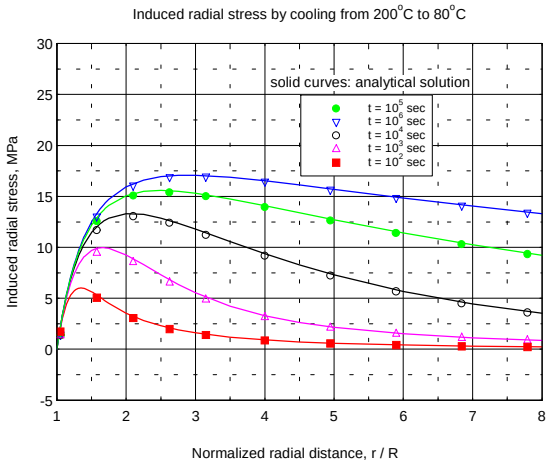

Figure 4: Radial stress distribution around the wellbore.

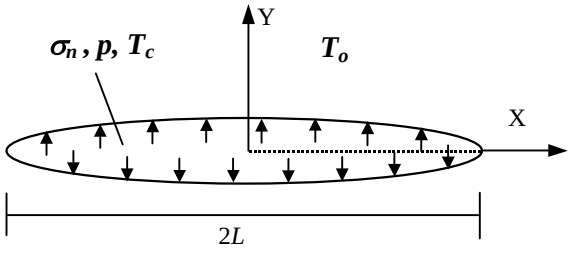

Figure 5: Uniformly pressurized, cooled crack.

steady-state thermal stresses that are generated by a heat sink to the surfaces of a Griffith crack. For a two dimensional geometry (plane strain) it can be shown analytically that the stresses induced on the fracture faces (at steady-state) are given by:

$$\sigma_{xx} = \sigma_{yy} = \frac{\beta_s E \Delta T}{6(1-\nu)} \qquad (13)$$

and equal 40 MPa for a crack in Westerly Granite. This stress will cause a significant reduction in the effective stress acting on natural fractures causing fractures to open and to slip under tectonic stresses thus increasing fracture permeability.

We now present some applications of the numerical models to the Coso geothermal field. We first consider wells **38A-9** and **38B-9** and study the stress distributions and the potential for drilling-induced fractures around them

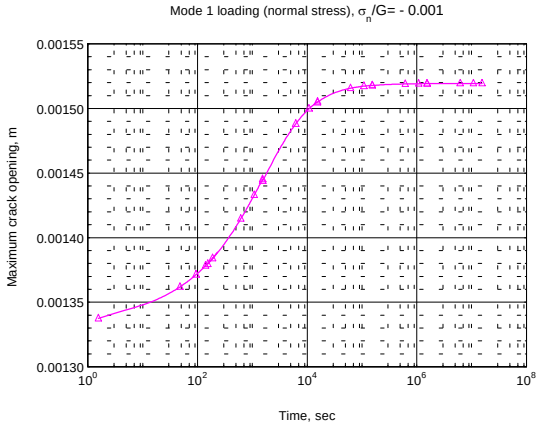

Figure 6: Crack opening as a result of stress applied to its surface.

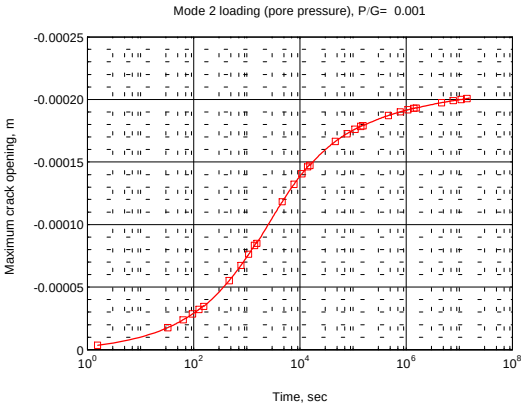

Figure 7: Crack closure resulting from a fluid pressure diffusion into the rock.

at a depth of 5000 ft and 7800 ft., respectively. In doing this, we consider two possible estimates of the in-situ stress magnitudes and directions as reported in the preliminary study of Sheridan *et al.* 2003 namely (normal and strike slip faulting regimes). It is assumed that the principal stresses are parallel to the x- and y-coordinate axis and the well pressures are 16.5 and 25.81 MPa. Figures 9-10 show that after 10 hours of cooling significant tensile effective stresses develop around the well **38A-9** for both stress regimes. Similar results are observed for the other well (not shown). This has implications for wellbore stability as well as stimulation/injection op-

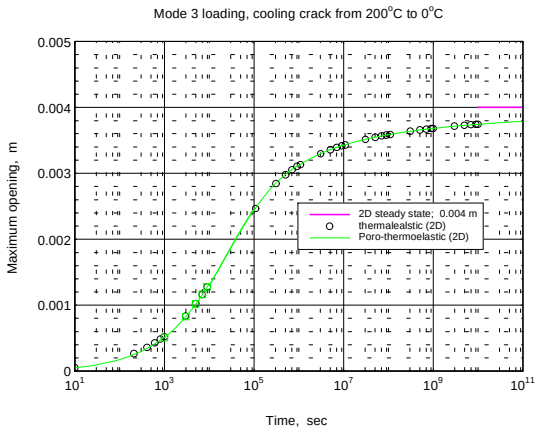

Figure 8: Crack opening caused by uniform cooling of the crack surfaces.

erations. These results are in agreement with the borehole image data from FMS surveys (Sheridan *et al.* 2003) that indicate the presence of drilling induced cracks and the absence of compressive type breakouts. One can expect similar results (induced tensile stresses) for well **83-16** when it is injected with cold water. The tensile stresses lead to fracturing which in turn enhances permeability and increases injection rate.

CONCLUSIONS

Transient porothermoelastic boundary element methods were used to study wellbore and crack problems to demonstrate some fundamental mechanisms associated with pressurization and cooling of the rock. The results presented illustrate the importance of the role of temperature in hydraulic fracture initiation and wellbore failure. Cooling of the rock near the wellbore reduces the total stresses (since radial stress at the well is constant, the stress difference, i.e., Mohr's circle radius is reduced) and induces a pore pressure drop inside the formation that increases the effective stresses near the wellbore. As time increases, the mud temperature will equilibrate with its surroundings so that the formations higher in the section being drilled are subjected to the increased temperature of the mud. Heating increases pore pressure and total stresses near the wellbore, the former reduces the effective stresses.

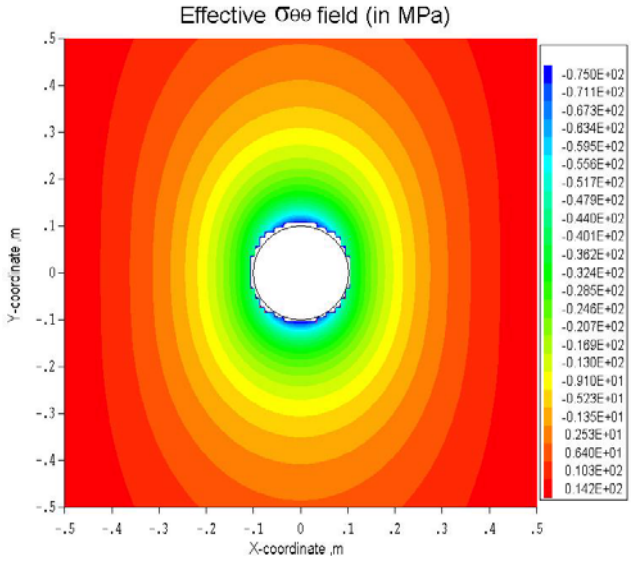

Figure 9: Well 38-9A, normal faulting regime, 5000 ft.

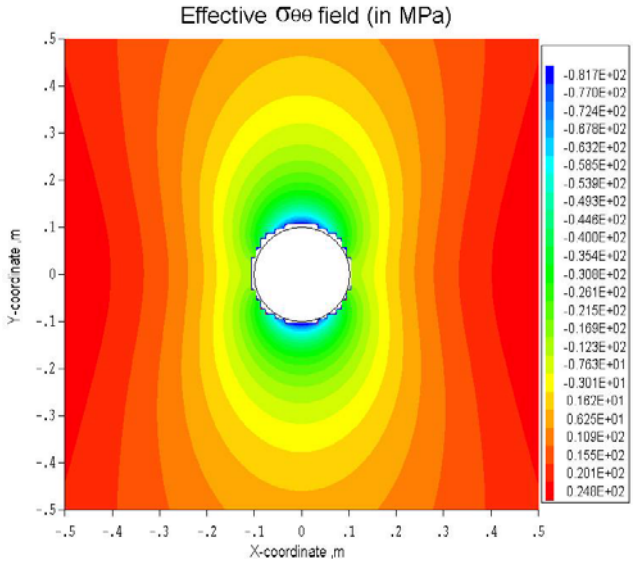

Figure 10: Well 38-9A, reverse faulting regime, 5000 ft.

The heating and cooling processes may be occurring simultaneously in the lower and upper segments of the wellbore, respectively. Cooling causes wellbore stability with respect to shear failure and instability with respect to tensile failure. The latter mechanism is useful in fracture initiation in stimulation; it also significantly enhances fracture permeability. Cooling increases the stress intensity at the fracture tip leading to crack growth, the latter will be further investigated in the future using the displacement discontinuity method. The results also show that cold fluid injection in the reservoir can alter the stresses significantly and reduce the effective normal stress on joints. As a result, fracture slip is highly likely and can lead to permeability enhancement.

ACKNOWLEDGMENTS

The financial support of the U.S. DOD (N68936-02C0214) and University of North Dakota Faculty Seed Money Program are gratefully acknowledged.

REFERENCES

Biot, M.A. 1941. General theory of three-dimensional consolidation. *J. Applied Physics,* 26: 182-185.

Cheng A.H.-D, Ghassemi, A., Detournay, E., 2001. A two-dimensional solution for heat extraction from a fracture in hot dry rock. *Int. J. Numerical & Analytical Methods in Geomechanics*, 25: 1327-1338.

Crouch, S.L, Starfield, A.M., 1983. *Boundary element methods in solid mechanics*. Allen Unwin.

Delaney, P.T., 1982. Rapid intrusion of magma into wet rock: groundwater flow due to pore pressure increases. *J. Geophys. Research,* 87(B9): 7739-7756.

Detournay, E., Cheng, A.H.-D.. 1991. Plane strain analysis of a stationary hydraulic fracture in a poroelastic medium. *Int. J. Solids & Structures*, 37(13): 1645–1662.

Ghassemi, A., Zhang, Q., 2004. A transient Fictitious Stress Boundary Element Method for Poro-thermoelastic Media. *J. Eng. Anal. Boundary Elements* (in press).

Ghassemi, A., Tarasovs, A., Cheng, A.D.-H., 2003. An Integral equation method for modeling three-dimensional heat extraction from a fracture in hot dry rock. *Int. J. Num. & Anal. Methods in Geomech.*, **27**, No. 12, 989-1004.

Ghassemi, A., Diek A., 2002. Poro-thermoelasticity for Swelling Shales. *J. Pet. Sci & Engineering*, 34: 123-135.

Ghassemi, A., Cheng, A.H.-D, Diek, A., Roegiers J.-C., 2001. A complete plane- strain fictitious stress boundary element method for poroelastic media. *J. Eng. Analysis with Boundary Elements*, 25(1): 41-48.

Ghassemi, A., Roegiers, J.-C., 1996. A three-dimensional poroelastic hydraulic fracture simulator using the displacement discontinuity method. *Proc. 2nd North American Rock Mech. Symposium*, 1: 982-987.

Li X., Cui, L., Roegiers, J.-C., 1998. Thermo-poroelastic modeling of wellbore stability in non-hydrostatic stress field. *Int. J. of Rock Mech. & Min. Sci.,* 35(4/5): Paper No. 063.

McTigue, D.F., 1986. Thermoelastic response of fluid-saturated porous rock, *J. Geophys. Research,* 91(B9): 9533-9542.

Palciauskas, V.V., Domenico, P.A., 1982. Characterization of drained and undrained response of thermally loaded repository rocks, *Water Resources Research*, 18: 281-290

Sheridan, J., Kovac, K., Rose, P., Barton, C., McCulloch, J., Berard, B., Moore, J., Petty, S., Spielman, P., 2003. In Situ Stress, Fracture and Fluid Flow Analysis-East Flank of the Coso Geothermal Field. 28th Stanford Geothermal Workshop, California.

Wang, Y., Papamichos, E., 1994. Conductive heat flow and thermally induced fluid flow around a well bore in a poroelastic medium. *Water Resources Research*, 30(12)**:** 3375-3384.

Williams, H., and McBirney, A.R., 1979. *Volcanology*, Freeman Cooper, San Francisco, CA.

Zhang, Q., 2004. Transient Poro-thermoelastic Boundary Element Methods with Rock Mechanics Applications. M.S. Thesis. University of North Dakota.